PCT/GB99/03417

The Patent Office

09/807395

INVESTOR IN PEOPLE

GB99/3417

4

The Patent Office
Concept House
Cardiff Road
Newport
South Wales
NP10 8QQ

I, the undersigned, being an officer duly authorised in accordance with Section 74(1) and (4) of the Deregulation & Contracting Out Act 1994, to sign and issue certificates on behalf of the Comptroller-General, hereby certify that annexed hereto is a true copy of the documents as originally filed in connection with the patent application identified therein.

In accordance with the Patents (Companies Re-registration) Rules 1982, if a company named in this certificate and any accompanying documents has re-registered under the Companies Act 1980 with the same name as that with which it was registered immediately before re-registration save for the substitution as, or inclusion as, the last part of the name of the words "public limited company" or their equivalents in Welsh, references to the name of the company in this certificate and any accompanying documents shall be treated as references to the name with which it is so re-registered.

In accordance with the rules, the words "public limited company" may be replaced by p.l.c., plc, P.L.C. or PLC.

Re-registration under the Companies Act does not constitute a new legal entity but merely subjects the company to certain additional company law rules.

PRIORITY DOCUMENT
SUBMITTED OR TRANSMITTED IN COMPLIANCE WITH RULE 17.1(a) OR (b)

Signed

Dated 15.11.99

Patents Form 1/77

Patents Act 1977
(Rule 16)

The Patent Office

1/77

15OCT98 E397287-1 D02697
P01/7700 0.00 - 9822397.7

Request for grant of a patent

(See the notes on the back of this form. You can also get an explanatory leaflet from the Patent Office to help you fill in this form)

The Patent Office

Cardiff Road
Newport
Gwent NP9 1RH

1. Your reference

PA/GX98

THE PATENT OFFICE
L
15 OCT 1998
RECEIVED BY POST

2. Patent application number
(The Patent Office will fill in this part)

9822397.7

3. Full name, address and postcode of the or of each applicant *(underline all surnames)*

KUI MING CHUI
8 GILBEY CLOSE
ICKENHAM
UXBRIDGE
MIDDLESEX UB10 8TD

Patents ADP number *(if you know it)*

If the applicant is a corporate body, give the country/state of its incorporation

06333546001

4. Title of the invention

IMAGING

5. Name of your agent *(if you have one)*

GRAHAM F COLES

"Address for service" in the United Kingdom to which all correspondence should be sent *(including the postcode)*

GRAHAM COLES & CO
24 SEELEYS ROAD
BEACONSFIELD
BUCKINGHAMSHIRE
HP9 1SZ

Patents ADP number *(if you know it)*

~~4361556001~~ 06787220001

6. If you are declaring priority from one or more earlier patent applications, give the country and the date of filing of the or of each of these earlier applications and *(if you know it)* the or each application number

Country	Priority application number *(if you know it)*	Date of filing *(day / month / year)*

7. If this application is divided or otherwise derived from an earlier UK application, give the number and the filing date of the earlier application

Number of earlier application	Date of filing *(day / month / year)*

8. Is a statement of inventorship and of right to grant of a patent required in support of this request? *(Answer 'Yes' if:*

a) any applicant named in part 3 is not an inventor, or
b) there is an inventor who is not named as an applicant, or
c) any named applicant is a corporate body.
See note (d))

NO

9. Enter the number of sheets for any of the following items you are filing with this form. Do not count copies of the same document

Continuation sheets of this form	
Description	27
Claim(s)	
Abstract	
Drawing(s)	8 + 8

10. If you are also filing any of the following, state how many against each item.

Priority documents	
Translations of priority documents	
Statement of inventorship and right to grant of a patent *(Patents Form 7/77)*	
Request for preliminary examination and search *(Patents Form 9/77)*	
Request for substantive examination *(Patents Form 10/77)*	
Any other documents *(please specify)*	

11. I/We request the grant of a patent on the basis of this application.

Signature [signature] Date 14/10/98

12. Name and daytime telephone number of person to contact in the United Kingdom GRAHAM F COLES ☎ 01494 677181

Warning

After an application for a patent has been filed, the Comptroller of the Patent Office will consider whether publication or communication of the invention should be prohibited or restricted under Section 22 of the Patents Act 1977. You will be informed if it is necessary to prohibit or restrict your invention in this way. Furthermore, if you live in the United Kingdom, Section 23 of the Patents Act 1977 stops you from applying for a patent abroad without first getting written permission from the Patent Office unless an application has been filed at least 6 weeks beforehand in the United Kingdom for a patent for the same invention and either no direction prohibiting publication or communication has been given, or any such direction has been revoked.

Notes

a) *If you need help to fill in this form or you have any questions, please contact the Patent Office on 0645 500505.*

b) *Write your answers in capital letters using black ink or you may type them.*

c) *If there is not enough space for all the relevant details on any part of this form, please continue on a separate sheet of paper and write "see continuation sheet" in the relevant part(s). Any continuation sheet should be attached to this form.*

d) *If you have answered 'Yes' Patents Form 7/77 will need to be filed.*

e) *Once you have filled in the form you must remember to sign and date it.*

f) *For details of the fee and ways to pay please contact the Patent Office.*

Imaging

This invention relates to imaging.

The invention is concerned especially with imagining techniques using CT (computed tomography), otherwise known as CAT (computer assisted tomography), scanning.

CT scanning provides an image that may be displayed on a monitor, of a transverse slice of the head or body of a patient. A polychromatic X-ray source of 100 KeV to 140 KeV is used for penetration of the patient and the image is derived from reconstruction within a fast data-processor of sample data collected from a detector array system. The CT contrast number for each voxel of the CT image is expressed in terms of the ratio of the difference in the X-ray linear attenuation coefficient of the tissue from that of the water within the voxel, with respect to that of the water, scaled to 1000.

In order to optimise the integrated X-ray dose received by the patient, and to obtain a reasonable signal-to-noise ratio in the image, the sampling is carried out in accordance with elongate voxels having their longer axis normal to the plane of the slice. As a consequence, high spatial resolution images are produced only in the transverse plane, and reconstruction in oblique or otherwise non-transverse planes provides poor spatial resolution.

A system of radiotherapy-treatment planning (RTP) based on CT imaging and called the "EMI Plan", has been used in hospitals for many years. However, owing to the inherently poor spatial resolution provided by CT for reconstructed images in the non-transverse planes, only two-dimensional RTP using CT, namely RTP(CT), is

possible. The basic technology used has changed little over the years and the limitation on effective imaging to allow other than two-dimensional RTP(CT), has remained.

Two-dimensional RTP(CT) has disadvantages which arise from limitation of the number of X-ray beam paths that can be used, and errors in CT-number computation arising from the elongate form of the voxels used for sampling. More particularly, there is a theoretical maximum of four for the number of paths for X-ray beams that can be used without creating beam-overlap outside the area to be treated; the accumulated dose is required to be as high as possible throughout the area to be treated and as small as possible in the healthy tissue surrounding, outside this area. Also, because elongated voxels are used for the CT scans, there is a partial-volume effect, especially along the edges of a lesion, which in general leads to lack of clarity and precision in the reconstructed image, impairing visual diagnosis and computation of the isodose curves.

It is an object of the present invention to provide a method of imaging, and an imaging system, of improved form as compared with the methods and systems currently used, such as to enable improvement in diagnosis and therapy to be achieved.

According to one of the aspects of the present invention there is provided a method of imaging wherein corresponding computed tomography (CT) and magnetic resonance (MR) scans of the same part of a subject are derived, the scans are related to one another for correlation of one to the other positionally with respect to said part using a de-convolution mapping process, and imaging of said part of the subject is provided in accordance with the MR scan as modified at different locations along its length spatially in dependence upon

the CT contrast numbers applicable to the corresponding, correlated locations of the CT scan.

According to another of the aspects of the present invention there is provided an imaging system comprising means for deriving corresponding computed tomography (CT) and magnetic resonance (MR) scans of the same part of a subject, means for relating the scans to one another for correlation of one to the other positionally with respect to said part using a de-convolution mapping process, and means for providing imaging of said part of the subject in accordance with the MR scan as modified at different locations along its length spatially in dependence upon the CT contrast numbers applicable to the corresponding, correlated locations of the CT scan.

With CT, signal magnitude is monitored by the attenuation of the polychromatic X-ray photon energy by all the atoms within the beam path. The linear attenuation coefficient, μ, is dependent on the density of the absorber and the atomic numbers of the atoms in the X-ray beam path, and contrast numbers relative to water on an absolute scale are derived. However, MR makes use of signals derived from the so-called 'T1-weighted' and 'T2-weighted' protons of quantum processes, and has contrast numbers that are relative in scale. The MR contrast numbers are accordingly uncorrelated with those for CT. This lack of correlation is confirmed by consideration of bone and water which are at opposite ends of the CT contrast (absolute) scale, but which are at the same end of the MR-image contrast (relative) scale owing to their common low proton-population.

The lack of correlation between the CT and MR signals acts against their use in combination for imaging purposes, but the present invention provides a method and

system by which the advantages of each may be utilised to improve image resolution and contrast information.

In the latter regard, CT provides a high spatial resolution but only in regard to view normal to the transverse slice. Resolution for all re-constructed non-transverse planes is poor owing to the need to use elongate voxels to improve signal-to-noise ratio. Also, the partial-volume effect of using elongate voxels may give rise to detection errors at the thin edge of a contrast profile of a lesion. MR, on the other hand, can give the same high degree of spatial resolution viewed in the normal direction to any image-slice plane, and can also provide isotropic resolution with cubic-voxel volume imaging.

A method of imaging, and an imaging system, in accordance with the present invention will now be described, by way of example, with reference to the accompanying drawings, in which:

Figure 1 is a flow diagram illustrating the method, and by implication the system also, of the present invention;

Figures 2 and 3 show diagrammatically for the purposes of explanation of the invention, translation from an object domain to an image domain, and a process of convolution and de-convolution, respectively;

Figure 4 illustrates relationships between waveforms represented respectively at (a) in real space, at (b) in image space and at (c) in de-convolution space;

Figures 5 and 6 illustrate, respectively, one-dimensional and two-dimensional generation of de-convolution maps;

Figures 7 to 9 show respectively in perspective, plan and side elevation, a form of couch-top used in the method and system of the invention;

Figures 10 and 11 show in perspective and cross-section, respectively, a form of cylindrical drum phantom for use in the method and system of the invention;

Figures 12 and 13 show in perspective and cross-section, respectively, a form of elliptical drum phantom for use in the method and system of the invention;

Figures 14 and 15 are cross-sectional views of cylindrical and elliptical drum phantoms that may be used as alternatives to those of Figures 10 to 13;

Figure 16 is illustrative of signal waveforms derived during the method of the invention; and

Figure 17 illustrates graphical representation derived from the signals of Figure 16.

In the method of the invention, as indicated in Figure 1, multiple-slice transverse CT scans are collected across a section of the volume of interest in a patient or other subject. Corresponding multiple-slice transverse MR scans of the same volume are collected correspondingly. The slice thickness of the latter scans may be one half, or smaller, of the thickness of the CT slices, and may be collected two-dimensionally or three-dimensionally. The patient is constrained throughout on a couch that provides landmarks with respect to a coordinate reference arrangement on the couch-top. This is to ensure the reproducibility of anatomical positions and features to the first order accuracy for the corresponding CT and MR scans, and also for the final radiation treatment to be made.

The respective transverse planes of the CT and MR images are processed individually in the method and are matched with one another in a de-convoluted space for the CT and MR images, as later explained. The two sets of de-convoluted maps are then merged together to a second order of accuracy in order that the CT numbers may be transferred over to replace the corresponding MR contrast numbers. Once this has been achieved, non-transverse (or oblique) planes can be obtained from the two-dimensional (2D) MR images or from the re-arrangement of the corresponding voxels of the three-dimensional (3D) volume images; where a 2D-MR is used, a further step of contrast transformation may be required.

In CT the transmitted beam intensity I is given by:-

$$I = I_0 \exp[-\mu(x,y)ds] \quad .. (1)$$

where: I_0 is the incident beam intensity; and
μ is the linear attenuation coefficient, which is dependent on the density of the absorber (e.g. tissue) and the atomic numbers of the atoms in the beam path.

The integral, ie $\Sigma\mu(x,y)ds$, of equation (1) along a ray path through the whole body tissue gives the ray sum or the ray projection, p where:

$$p = - \ln (I/I_0) \quad .. (2)$$

The reconstruction to build up each pixel value in CT number is by 'back-projection' and over-lapping of ray projections of all the different angles sampled in a data collection. The CT number is given by the expression:

$$[\{(\mu(\text{tissue}) - \mu(\text{water})\}/ \mu(\text{water})] \times 1000 \quad .. (3)$$

By adding the effect of the inverse-square law to equation (1) above, the percentage dose at depth d below the skin surface, for RTP is given by the expression:

$$[\{f^2 \times \exp(-\mu d)\}/(f + d)^2] \times 100 \quad .. (4)$$

where: f is the focus to skin distance (FSD) for the photon beam; and
μ is the linear attenuation coefficient at the photon energy of the radiotherapy beam.

A polychromatic photon energy spectrum is used in both CT and RTP for equations (1) and (2) and expression (4).

Further in relation to CT, the mass attenuation coefficient μ/ρ, where ρ is the density of the absorber, is given by:

$$\mu/\rho = \mu_e/\rho + \tau/\rho + \sigma/\rho + \pi/\rho \quad .. (5)$$

where: μ_e/ρ is the mass attenuation coefficient for elastic scattering, given by:

$$\mu_e/\rho \propto Z^2/E \quad .. (6)$$

for which Z is the atomic number of the absorber and E is the energy of the photon (the process involves scattering without absorption in the medium, and owing to the low Z in biological tissues, μ_e/ρ is negligible);
τ/ρ is the mass attenuation coefficient for the photoelectric absorption for which:

$$\tau/\rho \propto Z^3/E^3 \quad .. (7)$$

up to about 200 KeV, and at higher energies, E^3 approximates to E^2 and eventually to E (in the low energy region, the mass attenuation coefficient is about equivalent to the mass absorption coefficient, and the strong dependency on the atomic number of the tissue is the reason for the clear contrast between bones and other tissues in X-ray radiography and CT imaging - which uses an X-ray beam of about 100 KeV - 140 KeV);
σ/ρ is the mass attenuation coefficient for Compton scattering and absorption:-

$$\sigma/\rho \propto (\text{electron density})/E \quad .. (8)$$

for which electron density = N(A) x Z/A

N(A) being Avogadro's number, Z atomic number and A atomic mass number and:

$$\sigma/\rho = \sigma_s/\rho + \sigma_a/\rho \quad .. (9)$$

σ_s/ρ being the loss by the scattered photon, and σ_a/ρ an absorption loss which is due to the energy transmitted to the 'recoiled' electron and hence to the medium itself (the energy carried away by scattered photons is on average greater below 1.5 MeV, whereas the absorption by 'recoiled' electrons is greater above this); and

π/ρ is the mass attenuation coefficient for pair production:-

$$\pi/\rho \propto (E-1.02) \times Z \quad .. (10)$$

for which π is mainly the absorption of energy carried away by two 'annihilation' photons of 0.511 MeV at the photon energy of 1.02 MeV or greater.

MR imaging is related to the magnetic moments of nuclei (such as the protons of the abundant water molecules and tissue proteins present in the body) in precession about a uniform magnetic field, B0. This is governed by the Larmor Equation:

$$w_0 = \gamma \times B0$$

where w_0 is the angular frequency of the precessing nuclei, and γ is the magnetogyric ratio of the nuclei.

The T1-weighted relaxation relates to the application of radio frequency (RF) to cause the magnetic moments of nuclei to be excited to a higher energy quantised state. When the RF energy is switched off, the excited nuclei return to their lower energy state, releasing the absorbed energy; this releasing process, identified as the T1-weighted relaxation, restores the longitudinal magnetisation (spin-lattice interaction between the nucleus and its environment). In practice, the T1-

weighted relaxation is measured using an RF field that is applied orthogonally to the B0 field to rotate the precessing nuclei through either 90 degrees (saturation recovery), or more suitably, 180 degrees followed by a further 90 degrees (inversion recovery). Detection in each case may be from spin echo response or free induction decay (FID).

The T1-weighted signal derived from the nucleus in tissue, is given by:

(i) using saturation recovery:

(a) from spin-echo:

$$\rho = \rho_\phi[1-\exp(-\{t_R-TE\}/T1)][\exp(-TE/T2)] \quad .. \text{ (11a)}$$

where: t_R is the repetition time of the successive pulse sequences;
TE is the echo time (from the 90-degree pulse to the peak of the spin echo);
T1 is the spin-lattice relaxation time of the nucleus in tissue;
T2 is the spin-spin relaxation time of the nucleus in tissue;
ρ is the signal intensity (in arbitrary units); and
ρ_ϕ is the value of ρ at $t_R = \infty$ (but in practice, t_R may be finite).

(b) from FID - for which TE is zero reducing equation (11a) to:

$$\rho = \rho_\phi[1-\exp(-t_R/T1)] \quad .. \text{ (11b)}$$

or:

(ii) using inversion recovery

(a) from spin-echo:

$$\rho = \rho_\phi[1-\{2-\exp(-\{t_R-\tau-TE\}/T1)\}\exp(-\tau/T1)]\exp(-TE/T2) \quad ..(12a)$$

where: τ is the time between the 180-degree pulse and the following 90-degree pulse;

TE is the echo time (from the 90-degree pulse to the peak of the spin echo) equal to 2τ.
T1 is the spin-lattice relaxation time of the nucleus in tissue;
T2 is the spin-spin relaxation time of the nucleus in tissue;and
ρ_ϕ is the value of ρ at $t_R = \infty$ (but in practice, t_R may be finite).

(b) from FID - for which TE is zero reducing equation (12a) to:

$$\rho = \rho_\phi[1-2\exp(-\tau/T1)+\exp(-t_R/T1)] \quad .. \quad (12b)$$

The second type of signal decay arises from relaxation of the 'spin-spin' interaction or T2-weighted signal decay. The T2-weighted proton density and the relaxation in the signal decay may be measured by the 're-focused' or 're-clustered' echo-signal or signals. The formation of an echo arises if the nuclei are perturbed (or excited) from their equilibrium state (i.e. are rotated away from the alignment with the magnetic field, B0) by the application of a 90-degree pulse of RF energy. They initially all precess in phase with one another (i.e. they are coherent in phase) at the switching off of the RF energy, but with time they are affected by two processes, namely: (a) their spin-spin interaction, that is, the incremental-field interaction of one nucleus upon its neighbours and *vice versa*, and (b) the inhomogeneity of the main magnetic field B0 causing the nuclei to precess faster or slower at different locations so that phase coherence is lost as time progresses.

The dephasing effect of (b) can be corrected by applying a reverse (180-degree) RF pulse after an interval. This will reverse the precessing vectors of the nuclei, thus causing the 're-focusing' or 're-clustering' of the dispersing nuclei to re-establish a coherently-phased

signal. The initial transverse magnetisation is thus reduced only by the T2 decay, i.e. the spin-spin interactions as described in (a), and can be determined.

The T2-weighted signal magnitude of the nucleus in tissue is given by:-

$$\rho_k = \rho_\phi[1-\exp(-\{t_R-TE_{(n)}\}/T1)]\ \exp(-TE_{(k)}/T2) \quad .. \quad (13)$$

where: ρ_k is the signal intensity for the kth of n echoes (in arbitrary units);

TE is the overall time-of-echo, equal to 2τ where τ is the time between the 90-degree and 180-degree pulses;

$TE_{(n)}$ is the echo time for the nth echo (from the middle of the 90-degree pulse to the peak of the last spin-echo);

$TE_{(k)}$ is the echo time for the kth echo (from the middle of the 90-degree pulse to the peak of the kth echo);

T1 is the spin-lattice relaxation time of the nucleus in tissue;

T2 is the spin-spin relaxation time of the nucleus in tissue; and

ρ_ϕ is proportional to the signal from the population of nuclei within a voxel of tissue being imaged at $t_R = \infty$ (but in practice, t_R may be finite).

Other types of scan sequence may be used.

The following TABLE shows the relevant NMR properties of various nuclei.

In the TABLE: RA is percentage relative abundance;
RS is relative sensitivity at constant field for equal number of nuclei;
MTR is magnetogyric ratio (γ) in MHz per Tesla; and
LF is Larmor frequency in MHz at 1.5T.

TABLE

Nucleus	RA	RS	MTR(γ)	LF
1H	99.98	1.00	42.58	63.87
2H	0.015	9.65×10^{-3}	6.53	9.80
13C	1.11	0.016	10.71	16.07
19F	100.00	0.830	40.05	60.08
23Na	100.00	0.093	11.26	16.89
31P	100.00	6.60×10^{-2}	17.23	25.85
39K	93.1	5.08×10^{-4}	1.99	2.99

In human tissues, protons from water molecules and protein are abundant. The MR imaging technique makes use of the signals from the T1-weighted and T2-weighted protons. In the MR scan, the spatial distributions in the three dimensions, may be encoded by applying three linear gradient fields orthogonal to each other. They are generated by coils strategically placed with respect to other coils within the system. The RF energy is transmitted and received by the transmitter and receiver coils strategically placed with respect to the main magnetic field, and the gradient fields. The 2D-MR sampling uses 90-degree and 180-degree RF pulses for excitations with one slice-selection gradient, one phase-encode step gradient, one read (frequency encode) gradient to obtain a 2D-slice.

The functions of the gradients may easily be swapped over or mixed allowing the data collections for the various orthogonal or oblique slices to be sampled. Hence all these slices are equally-well defined in the spatial resolution. The three-dimensional volume imaging technique uses the non-selective RF hard pulse to excite the whole volume, two phase-encode step gradients in two dimensions, with a fixed read (frequency encode) gradient in the third dimension. This may provide cubic voxels which are isotropic in their spatial resolution.

A comparison between CT and MR systems can be summarised as follows:

(a) contrast information in images:-

(i) CT: Signal magnitude is monitored by the attenuation of the polychromatic X-ray photon energy by all the atoms within the beam path. The linear attenuation coefficient, μ, is dependent on the density of the absorber and the atomic numbers of the atoms. As indicated by expression (3), the CT number is given by the attenuation coefficient for tissue with reference to that of water to define an absolute scale.

(ii) MR: T1- or T2-weighted signal decays of a quantum process from a selection of nuclei, e.g. mainly from protons owing to their relative sensitivity and their abundance in tissues (see the Table above). The signal magnitudes are expressed by equations (11)-(13). The contrast numbers are relative in scale.

By comparing (i) and (ii), it is quite obvious that the contrast numbers for CT and MR are uncorrelated. This is clear from consideration of bone and air which are at the two opposite extreme ends of the CT contrast scale related to water as the base line, but which are at the same end of the MR contrast scale owing to their common lack of proton population. Moreover, the CT contrast number is absolute whereas the MR contrast number is relative.

(b) spatial resolution:

(i) CT: High spatial resolution viewed in the normal direction to an image slice plane, is achievable only for the transverse slice. All re-constructed, non-transverse planes are poor in resolution owing to the elongated voxel size used in CT because of the constraints of minimising accumulated dose and poor signal-to-noise ratio. The partial-volume effect of the

elongate voxels also gives rise to detection errors at the thin edge of a contrast profile of a lesion.

(ii) MR: The same degree of high spatial resolution viewed in the normal direction to any image slice plane is obtainable by the switching/swapping of gradient fields for 2D-MR imaging. An isotropic resolution of a cubic-voxel image may be achieved in 3D-MR imaging.

(c) motion problems:

(i) CT: Owing to its fast scan, motion blurring in the image is arrested.

(ii) MR: Needs longer scan-time, so is therefore more prone to motion-blurring problems in images. When motion-suppressed scan sequences or fast scans (such as the echo planar imaging (EPI) described in GB-A-2235779) are developed and used, the motion artefacts can also be arrested as in CT; gating may also be used to help.

(d) geometrical distortion:

(i) CT: This is linear spatially, with no geometrical distortion.

(ii) MR: Geometrical distortions may result from an inhomogeneous magnetic field, B0, and/or non-linear impurity in one or more of the gradient fields. These distortions may be corrected by the use of scan sequences and/or phantoms.

The provision of 3D-RTP has significant advantages. With 3D there are theoretically up to twelve beam paths for treatment. This greatly improves the absorbed-dose ratio, that is to say, the ratio between the dose absorbed by the treated area to that absorbed by the surrounding healthy tissue, and also provides more options for the treatment-beam paths. Accordingly, it is possible to achieve a higher rate of successful treatment without serious damage to surrounding tissue or vital organs; the possible 300% improvement in the absorbed-

dose ratio should provide a better treatment success rate.

The use of MR images in 3D-RTP has the advantage that it makes high spatial resolution available in all planes, and reduces the partial volume effect. Furthermore, the use of electronic switching for field variation in MR, enables a thinner slice of the 2D orthogonal or oblique plane, or cubic-voxel 3D volume, to be achieved. The combined effect of all the above advantages markedly improves the overall diagnosis and treatment success rates.

3D-RTP is not possible using CT in that CT high spatial resolution is obtainable only in the transverse plane and that resolution in reconstructed non-transverse planes is poor giving rise to difficulties with both diagnosis and the calculation of isodose curves. But, and in accordance with the invention, 3D-RTP(MR) becomes a practical possibility because MR provides high spatial resolution in all planes. The MR contrast numbers in the 2D- or 3D-MR images are replaced by the corresponding CT contrast numbers, and steps are taken to overcome the geometrical-distortion and motion problems.

The method of the invention, and from this by implication the system by which the method is performed, is illustrated in the flow diagram of Figure 1. In the method, CT multiple-slice transverse (Tr) scans are collected across a section of the volume of interest in a patient. Similarly, corresponding MR multiple-slice transverse scans of one half, or smaller, of the slice thickness of the CT slices are collected across the same volume of interest by 2D-MR sampling or 3D-MR sampling.

The patient is constrained from movement during and between the two scanning processes on a universal couch-

top which also provides landmarks within a coordinate reference arrangement defined in the couch-top. The constraint and landmarking is necessary to ensure that anatomical positioning and features are maintained the same to a first order of accuracy for the CT and MR scans, and for the final radiation treatment. The respective transverse planes of CT and MR images are processed individually by using 'boundary' or 'finger-print' matching techniques in a de-convolution space (DCS) for the CT & MR images. The two sets of de-convoluted maps are then merged together to a second order of accuracy in order that the CT numbers may be transferred over to replace the corresponding MR contrast numbers. Once this has been done, non-transverse (or oblique) planes are obtained from the 2D-MR image or from the re-arrangement of the corresponding voxels of the 3D-MR volume; in the 2D-MR case, a further step of contrast transformation is required.

Geometrical distortion in the MR images may be corrected to a certain extent, by a combined spin-echo (SE) and field-echo (FE) scan sequence, with the SE part to correct for the field inhomogeneity in B0, and the FE part to overcome the impurity or non-linear gradients. The geometrical distortion may also be dealt with empirically using a post-process correction based on a set of phantom data relating to a drum phantom. Movement problems may be suppressed by some scan sequences and/or by gating; for certain parts of the body there is no movement problem for the MR scan.

Once the necessary sets of MR images with transferred CT numbers have been obtained, 3D-RTP may be started using the current 2D-RTP software package. The whole '3D-' space is covered through the use of several 2D planes in a pseudo-3D approach.

The results of the combined CT and MR method may be accumulated in a data bank so as to enable the technique to be performed in a so-called stand-alone MR method. For this method the X-tubing coordinate reference arrangement of the couch top is filled with a chemical solution, such as $MnCl_2$, of appropriate T1 and T2 values to establish a standard in the resulting MR image against which the other components of the image can be related. In this way, it is possible to standardise the contrast numbers of various types of tissue using a standardized 3D-RTP Scan Sequence. A data bank of standardised contrast numbers applicable to various tissues of different patients *versus* the CT numbers derived from the combined CT and MR method may then be accumulated over a period of time. The data, as 'banded' in the data base, may then be used to enable the stand-alone MR method to be performed. Interpretation may still be required by an operator or through an 'expert' system to overcome certain ambiguities (for example, in separating bone from air).

The matching technique is based on a method using de-convolution space (DCS) in combination with a least-squares curve-fitting method. These methods are separately well known in pure mathematics, but not, as in the present method and system, combined to produce de-convolution maps with the least-squares fitting curve used as a running filter. The filter is used to overcome practical difficulties due to noise within the image pixels.

For a mathematical model of the method, consideration is given to a line spread function (LSF) arising in the imaging system from an impulse or δ function; this is represented in Figure 2.

An example of the way in which the LSF of Figure 2 is convolved with an object step-down function to result in a roll-down edge response function (ERF), and how this through the de-convolution process reproduces the LSF, is illustrated in Figure 3. As illustrated, the LSF is a one dimensional profile across the edge of a contour with its peak position representing the 50%-level point of the ERF.

Figure 3 and the mathematical expressions set out below, indicate the way in which the LSF can be recovered from the resulting ERF at a contrast edge. For convolution related to points 1 to n of the step function:

at point 1:

$$\sum_{0}^{a} L(x)\,\Delta x = E(x)_1$$

at point 2:

$$\sum_{0}^{a} L(x)\,\Delta x - \sum_{a-1}^{a} L(x)\,\Delta x = E(x)_2$$

at point 3:

$$\sum_{0}^{a} L(x)\,\Delta x - \sum_{a-2}^{a} L(x)\,\Delta x = E(x)_3$$

until at point n:

$$\sum_{0}^{a} L(x)\,\Delta x - \sum_{1}^{a} L(x)\,\Delta x = E(x)_n$$

For de-convolution ie. for the ERF to manifest the LSF:

$$E(x)_1 - E(x)_2 = \sum_{a-1}^{a} L(x)\,\Delta x = L(x)_{(a-1)-a}\,\Delta x$$

thus:

$$\{E(x)_1 - E(x)_2\}/\Delta x = L(x)_{(a-1)-a}$$

$$\{E(x)_2 - E(x)_3\}/\Delta x = L(x)_{(a-2)-(a-1)}$$

leading to

$$\{E(x)_{(n-1)} - E(x)_n\}/\Delta x = L(x)_{(n-1)-n}$$

Thus, the same shape of LSF is recovered by the de-convolution process independently of the sense of the ERF; it does not matter whether a roll-up or a roll-down ERF of a positive or a negative contrast profile, is involved. This is an important property as a positive contrast contour will have roll-up (from low to high) ERFs at both ends whereas a negative contrast contour will have roll-down (from high to low) ERFs at both ends.

In the practical implementation, the LSF is derived from the ERF by de-convolution using a running filter. This enhances the accuracy of the method in overcoming the problem of noise that affects the digitised pixel values of the image. Use is made of a least-squares fitting of a set of data points that advances along the whole length of the function from one point to another.

Assuming that $y = a_0 + a_1x + a_2x^2$ represents the ERF curve a five-point or seven-point fit is used, and the normal equation becomes:

$$\begin{vmatrix} \Sigma 1 & \Sigma x_i & \Sigma x_i^2 \\ \Sigma x_i & \Sigma x_i^2 & \Sigma x_i^3 \\ \Sigma x_i^2 & \Sigma x_i^3 & \Sigma x_i^4 \end{vmatrix} \begin{vmatrix} a0 \\ a1 \\ a2 \end{vmatrix} = \begin{vmatrix} \Sigma y_i \\ \Sigma x_i y_i \\ \Sigma x_i^2 y_i \end{vmatrix}$$

where: i is 1+n, ... 5+n; ... until m-5, ... m
or
i is 1+n, ... 7+n; ... until m-7, ... m

n is 0,1, 2, ... ; and

1, ... m is the span of the ERF profile.

The solution may be derived from either:

$$\begin{vmatrix} a0 \\ a1 \\ a2 \end{vmatrix} = \begin{vmatrix} \Sigma 1 & \Sigma x & \Sigma x^2 \\ \Sigma x & \Sigma x^2 & \Sigma x^3 \\ \Sigma x^2 & \Sigma x^3 & \Sigma x^4 \end{vmatrix}^{-1} \begin{vmatrix} \Sigma y \\ \Sigma xy \\ \Sigma x^2 y \end{vmatrix} \quad .. (14)$$

or:

$$\frac{a0}{\begin{vmatrix} \Sigma y & \Sigma x & \Sigma x^2 \\ \Sigma xy & \Sigma x^2 & \Sigma x^3 \\ \Sigma x^2 y & \Sigma x^3 & \Sigma x^4 \end{vmatrix}} = \frac{a1}{\begin{vmatrix} \Sigma 1 & \Sigma y & \Sigma x^2 \\ \Sigma x & \Sigma xy & \Sigma x^3 \\ \Sigma x^2 & \Sigma x^2 y & \Sigma x^4 \end{vmatrix}} = \frac{a2}{\begin{vmatrix} \Sigma 1 & \Sigma x & \Sigma y \\ \Sigma x & \Sigma x^2 & \Sigma xy \\ \Sigma x^2 & \Sigma x^3 & \Sigma x^2 y \end{vmatrix}} = \frac{1}{\begin{vmatrix} \Sigma 1 & \Sigma x & \Sigma x^2 \\ \Sigma x & \Sigma x^2 & \Sigma x^3 \\ \Sigma x^2 & \Sigma x^3 & \Sigma x^4 \end{vmatrix}} \quad .. (15)$$

For both equations (14) and (15) to be valid:-

$$\begin{vmatrix} \Sigma 1 & \Sigma x & \Sigma x^2 \\ \Sigma x & \Sigma x^2 & \Sigma x^3 \\ \Sigma x^2 & \Sigma x^3 & \Sigma x^4 \end{vmatrix} \neq 0$$

The gradient at $dy/dx_{(3+n)}$ or $dy/dx_{(4+n)}$ can then be derived and plotted against x for the LSF profile.

The graph of dy/dx against x gives the LSF profile. The peak of this profile is located half way between the mid-points of the ascending and descending limbs of the graph and is derived from this as the so-called full-width-half-maximum (FWHM) with an accuracy to the sub-pixel level.

The point spread function (PSF) is the two dimensional profile which may be derived, in practice, from the two corresponding LSFs orthogonal to one another within an image plane. The peak position of the PSF profile is, therefore, from the 'mean' or 'cross-over' of the two

peaks or the two LSF profiles. The PSF is obtained in practice from two orthogonal axes in a two-dimensional plane.

The waveform relationships between real space (RS), image space (IS), and de-convolution space (DCS) are illustrated in Figures 4 at (a), (b) and (c) respectively. These show the relationship between peak positions p1, p2, p1′, p2′,p1" and p2" and dip positions d′ and d" in the DCS, with the positions and magnitudes of contrast value of the waveforms in the image space (IS) and real space (RS), and highlight certain useful properties of the process. In particular, the tail-end to tail-end distance of each LSF profile gives a spread of 100% down to 0%, and *vice versa*, in the corresponding ERF profile in IS. Also, the half way points of the full-width-half-maximum (FWHM) in the LSF profiles give the peak positions of p1, p2, p1′, p2′, p1", and p2" which correspond to the 50% level points of their related ERF profiles; the dip positions d′ and d" in the LSF profiles correspond to the central maxima or minima of the profiles in IS, and the distances of p1′ to p2′, and p1" to p2" correspond to the FWHMs of the profiles in the IS and the distances between the edges of the step function in RS.

From the above, the generation of the LSF (or PSF) is independent of the roll-up or roll-down nature of ERFs at the edges of the contrast contour. In other words, it is independent of the sense and the absolute value of the contrast numbers within the contour. The peak position of the LSF (or PSF) is the central half-way (50%) point of the roll-up or roll-down ERF which is the optimum position at which the two sets of ERFs are matched together with the overall effect of not distorting the contour shape within the boundary of the ERFs.

In order to match or merge together the two corresponding CT and MR images, they are transformed into DCS. In DCS the peaks of the LSFs (or PSFs) mark the central half-way points of the ERFs of the original two-dimensional image planes. These peak positions are then linked together to form the 'de-convolution' or 'finger-print' maps. Through the assistance of these maps, the two image files may now be matched or merged together to a second order of accuracy. Figures 5 and 6 illustrate one-dimensional and two-dimensional generation of de-convolution or finger-print maps in DCS.

The subsequent transformation of the contrast numbers is guided by a moving sub-set filter conformed by the sub-set mean values and the overall uniformity of the profile of the MR image; this filter is quite similar to the running filter used for the conversion of ERF to LSF. The number of samples in the moving sub-set filter may also be used for the cut-off rejection of small or 'point' contours, that is to say, spurious contours introduced by noise, within the CT or MR image.

A similar technique is employed for MR(Tr) to MR(Oblique) transformation of contrast numbers. Since a high spatial resolution and small partial volume effect are maintained for the thin 2D-MR(Oblique) slice or the 3D-MR(Oblique) plane, the transformation is relatively simple. Through this DCS technique, the high spatial resolution operation is maintained throughout the whole process of re-processing.

The combined MR and CT method of the invention requires the matching of corresponding CT and MR images with one another, and it is important that the same 'laid-out' features of anatomy are presented for the each scanning activity, and that the same features are presented again for radiation treatment. The couch-top is used for this

and the landmarks and reference axes defined in it are encoded into the images, for use as guides for the repositioning of the patient for any subsequent scanning or other activities, and also for the first order alignment in the initial matching of CT and MR images (allowing more refined matching to the second order of accuracy using the DCS technique, to be initiated).

The form of the couch-top will now be described with reference to Figures 7 to 9.

Referring to Figure 7 to 9, the couch-top has a flat upper part 100 that is carried by a curved lower part 101 which fits to the scanner table of the CT or MR installation. The patient lies on the flat part 100 and is constrained on it (by an arrangement not shown), so as to reproduce the same anatomical features for scanning and treatment; the treatment table similarly has a flat surface.

An X-tubing array 102 is embedded into the upper part 100. The tubing of the array 102 is of plastics or glass having an external diameter of up to 6 mm and an internal diameter of up to 3 mm, and is filled with a chemical solution of $MnCl_2$. The cross-sectional image of such tubing will show a positive profile for MR and a negative profile for CT. However, the DCS technique of processing these images pin-points their centres irrespective of the contrast values represented.

As shown in Figure 8, the patient is constrained by the constraint arrangement to lie lengthwise of the flat part 100 (ie along the z-axis of the coordinate system defined in the couch-top) and centrally of it (ie with respect to the lateral x-axis); the patient's head is placed on a head-rest 103 suitable for the scan, CT or MR, to be undertaken. Three landmarkers/constraint levers 104, two

under the armpits and one at the crotch between the thighs, are also used to position the patient as well as to provide some form of conformation with respect to the reference coordinate system. Air-compressed cushions (not shown) may be gently pressed in from either sides to conform the limbs and hence the body along its length.

The X-tubing array 102 inside the bottom flat part 100 may be used as the reference system for the transverse and sagittal planes, and the oblique planes between them. The flat surface of the part 100 or the flat contour of the patient's skin surface in contact with it may be used as the datum for the coronal planes. However, an extra small X-tubing array (not shown) may be placed above the patient using the three landmarkers as the supporting legs; this enables the small-angled oblique planes between the coronal and transverse planes to be monitored.

If the internal-bore diameter of the magnet of the MR scanner is large enough, an extra X-tubing array 105 (Figure 9) may be used along either side of the patient to help in monitoring the small-angled oblique planes between the coronal and sagittal planes. Furthermore, a curved X-tubing array (not shown) may be placed inside and on the bottom of the head rest (or head coil) 103 used for the MR scan for the purpose of clearly establishing the coordinates of the head.

The material of the couch-top is carbon fibre so as to ensure a low linear attenuation coefficient with transparency to X-rays. Edges of the couch-top are smoothly rounded to avoid sharp edges that would cause streaking in the CT image. Non-magnetic material is used throughout to avoid disturbing the uniform magnetic field, B0, used for MR.

The radiation treatment table needs to be capable of both translational, "in and out" movement as well as rotational movement to cover the 3D planning and treatment.

A final empirical correction of any residual geometrical distortion may be carried out using a cylindrical or elliptical drum phantom. A cylindrical drum phantom is illustrated in Figures 10 and 11, and an elliptical drum phantom in Figures 12 and 13.

Referring to Figures 10 and 11, the cylindrical drum phantom, which may be of about 160 mm in length and is for use with the head coil of the scanner, includes a central rod 200 of polymethyl methacrylate (as sold under the Registered Trade Mark PERSPEX) having a diameter of about 2 mm and defining the phantom centre, Cph. The body of the phantom is built up as concentric sections about the rod 200, each comprising evenly-spaced blocks 201 of polymethyl methacrylate and with the blocks 201 of each section in exact register radially with the gaps 202 between the blocks 201 of the preceding section. The central region 203, having a diameter of about 20 mm, may be left blank (since the magnetic field within the central region is uniform to within 0.1 ppm, so no B0 correction is required). The gaps 202 and the central region 203 are filled with an NMR solution (e.g. $MnCl_2$ or $CuSO_4$).

Peak positions of the PSFs in the DCS map for the drum are derived and stored. This data is then corrected for each point of the map with respect to the iso-centre of the scanner system, Ciso, using the following vector equation:-

$$\Delta r = r_2 - r_1$$

where Δr is the correction vector between Ciso and Cph; and
r_2 and r_1 are the vectors to the relevant point of the map from Ciso and Cph respectively.

The elliptical drum-phantom of Figures 12 and 13 is constructed in essentially the same manner as the cylindrical drum phantom, and is for use with the body coil of the scanner. The major and minor axes are chosen according to the field of view being studied.

As an alternative, the cylindrical and elliptical drum phantoms may be constructed as shown in Figures 14 and 15, using thin plates 300 of polymethyl methacrylate instead of the blocks used for the phantoms of Figures 10 to 13. The plates 300, which may have a thickness of between 1.5 mm and 2.0 mm, are spaced radially from one another by gaps 301 that, together with the central region 302 are filled with appropriate NMR solution.

CT scan images are not subject to geometrical distortion so CT scan data accumulated using the phantoms, and the DCS profile data consequently derived and stored, are used as a datum or reference set for correction of the MR scans. Such corrections also automatically correct for manufacturing tolerances, and the DCS data derived from the phantom through the CT and MR scans represents a reference situation devoid of motion.

The DCS technique described above is applicable further in diagnosis and treatment. In particular, it may be used to assist visual detection of gradual change of contrast level in scan images. For example, as illustrated in Figure 16, the 100% point at which the roll-off of a lesion profile begins can be readily plotted from the DCS profile, together with the 50%-level point, and then the 0% point where the profile has

completely levelled off. Graphic representations of these various points can then be plotted out to facilitate diagnosis, as illustrated in Figure 17, in the form of a string of characters 400 delineating the 100%-level, a string of characters 401 delineating the 50%-level and a string of characters 402 delineating the 0% level.

In current radiation treatment planning, a composite volume leaving a margin of 15 mm around a lesion, is used. To be effective, the tail-end of the lesion growth is to be within the treatment-beam path, and in this regard there is advantage in extending the DCS-profile plot of Figure 16 to include a point which is a distance (d) beyond the 0%-level. This is then used for diagnosis and treatment, to establish an outer string of characters 403 in the graphical representation of Figure 17. The distance (d) covers the penumbra-spread as well as any possible mis-alignment by the operator.

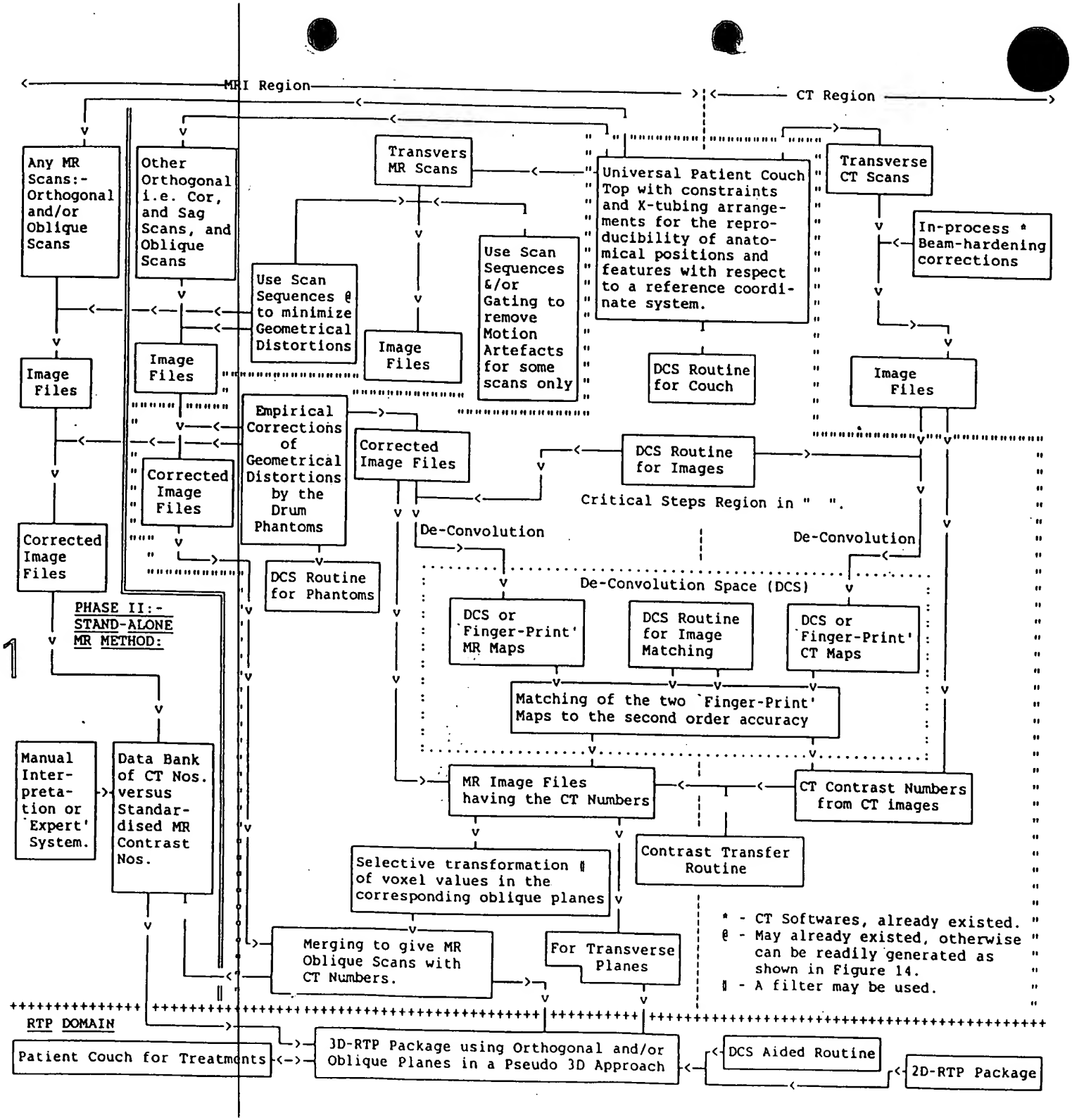
MRI Region
CT Region
Any MR Scans:- Orthogonal and/or Oblique Scans
Other Orthogonal i.e. Cor, and Sag Scans, and Oblique Scans
Transvers MR Scans
Universal Patient Couch Top with constraints and X-tubing arrangements for the reproducibility of anatomical positions and features with respect to a reference coordinate system.
Transverse CT Scans
In-process * Beam-hardening corrections
Use Scan Sequences @ to minimize Geometrical Distortions
Use Scan Sequences &/or Gating to remove Motion Artefacts for some scans only
Image Files
DCS Routine for Couch
Image Files
Image Files
Empirical Corrections of Geometrical Distortions by the Drum Phantoms
Corrected Image Files
DCS Routine for Images
Corrected Image Files
Critical Steps Region in " ".
Corrected Image Files
De-Convolution
De-Convolution
DCS Routine for Phantoms
De-Convolution Space (DCS)
PHASE II:- STAND-ALONE MR METHOD:
DCS or 'Finger-Print' MR Maps
DCS Routine for Image Matching
DCS or 'Finger-Print' CT Maps
Matching of the two 'Finger-Print' Maps to the second order accuracy
Manual Interpretation or 'Expert' System.
Data Bank of CT Nos. versus Standardised MR Contrast Nos.
MR Image Files having the CT Numbers
CT Contrast Numbers from CT images
Contrast Transfer Routine
Selective transformation ‖ of voxel values in the corresponding oblique planes
Merging to give MR Oblique Scans with CT Numbers.
For Transverse Planes
* - CT Softwares, already existed.
@ - May already existed, otherwise can be readily generated as shown in Figure 14.
‖ - A filter may be used.
RTP DOMAIN
Patient Couch for Treatments
3D-RTP Package using Orthogonal and/or Oblique Planes in a Pseudo 3D Approach
DCS Aided Routine
2D-RTP Package

Fig. 1

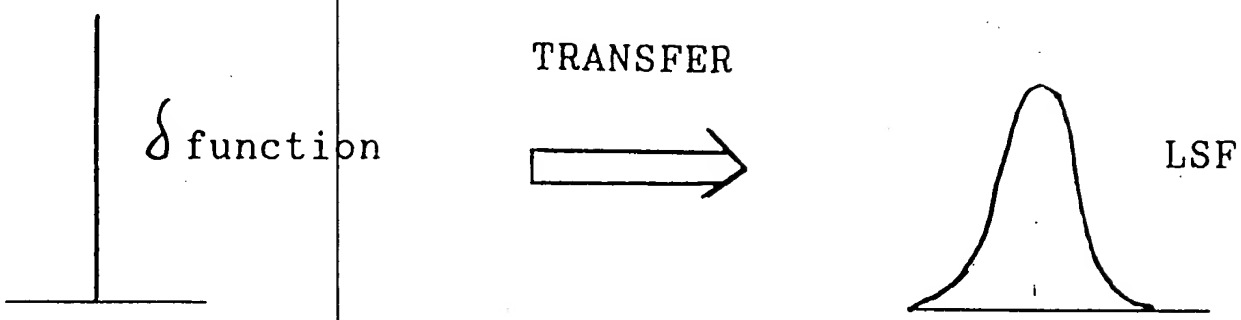
Object Domain
Image Domain
δ function
TRANSFER
LSF

Fig. 2

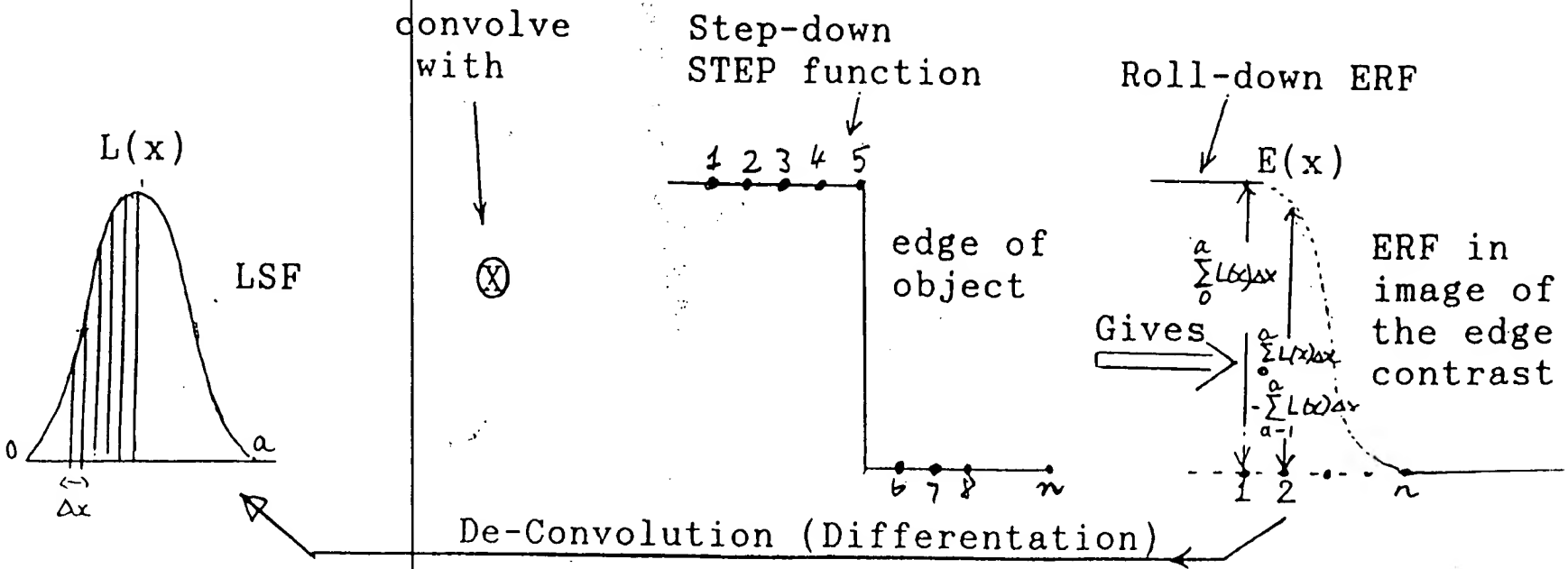
convolve with
Step-down STEP function
Roll-down ERF
L(x)
LSF
1 2 3 4 5
E(x)
edge of object
ERF in image of the edge contrast
Gives
De-Convolution (Differentation)

Fig. 3

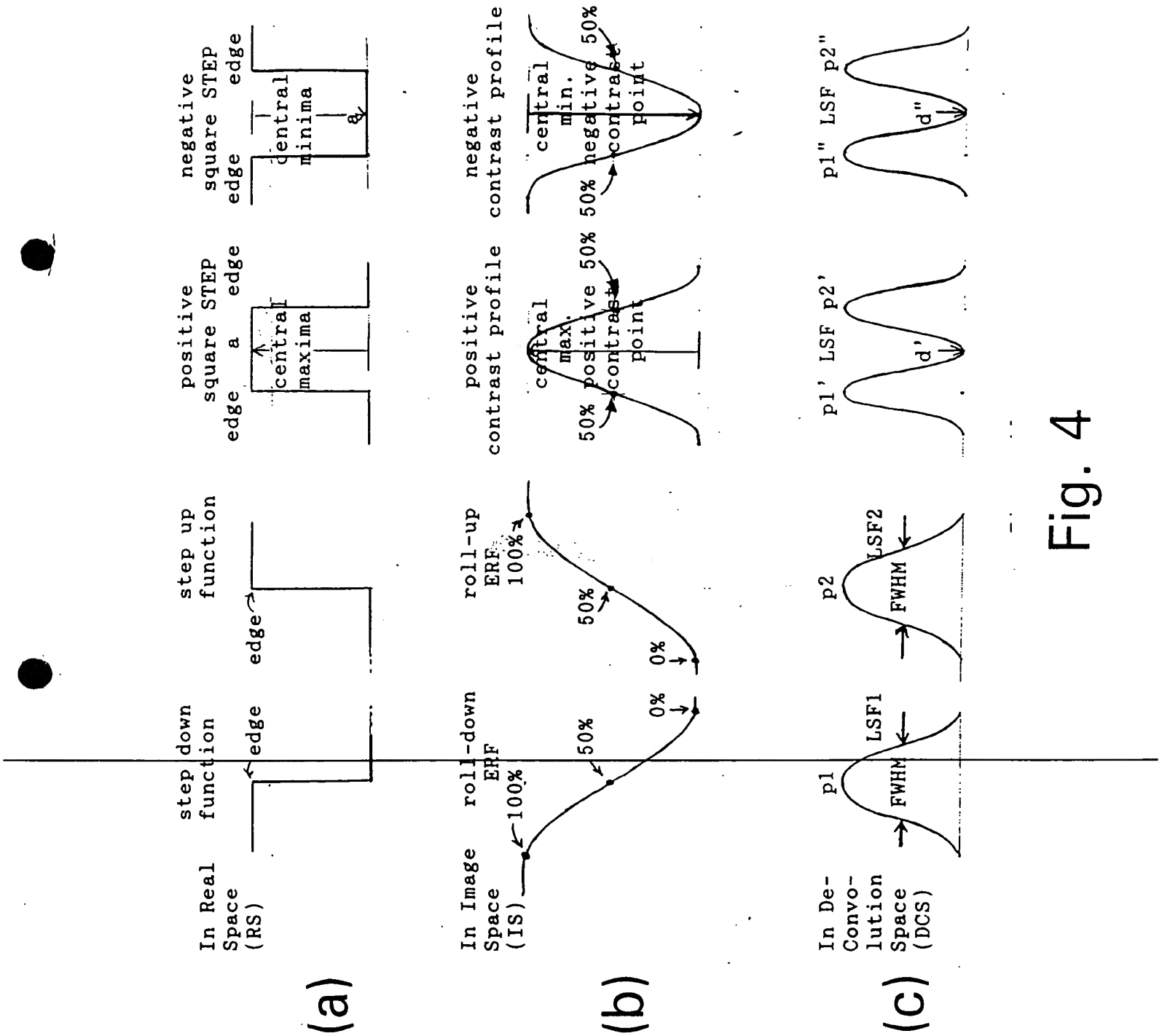
(a)
In Real Space (RS)
step down function
edge
step up function
edge
positive square STEP
edge
a
edge
central maxima
negative square STEP
edge
edge
central minima
a
(b)
In Image Space (IS)
roll-down ERF
100%
50%
0%
roll-up ERF
100%
50%
0%
positive contrast profile
central max.
50% positive contrast point
negative contrast profile
central min.
50% negative contrast point
(c)
In De-Convo-lution Space (DCS)
p1
LSF1
FWHM
p2
LSF2
FWHM
p1' LSF p2'
d'
p1" LSF p2"
d"

Fig. 4

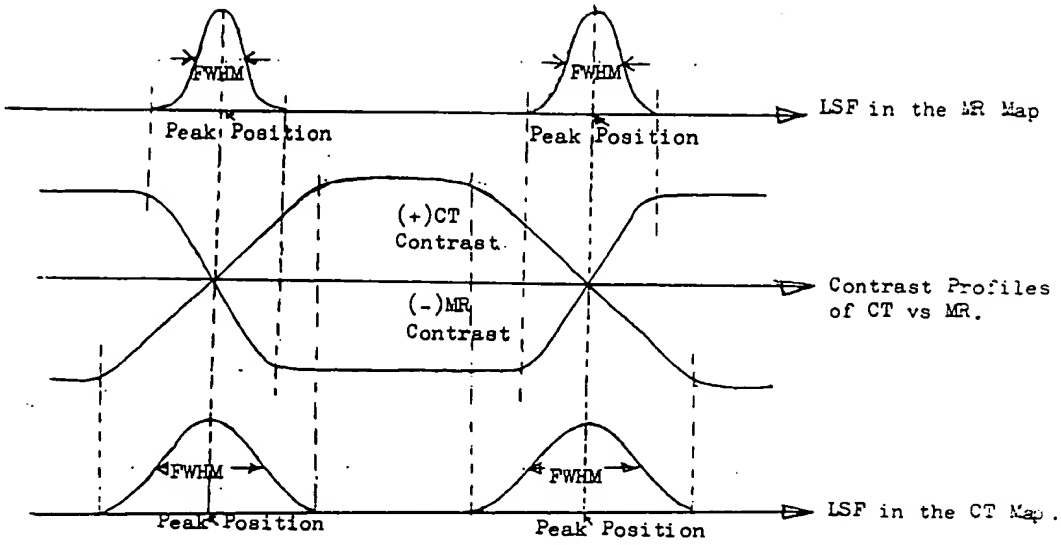
FWHM
FWHM
LSF in the MR Map
Peak Position
Peak Position
(+)CT Contrast
(-)MR Contrast
Contrast Profiles of CT vs MR.
FWHM
FWHM
LSF in the CT Map.
Peak Position
Peak Position

Fig. 5

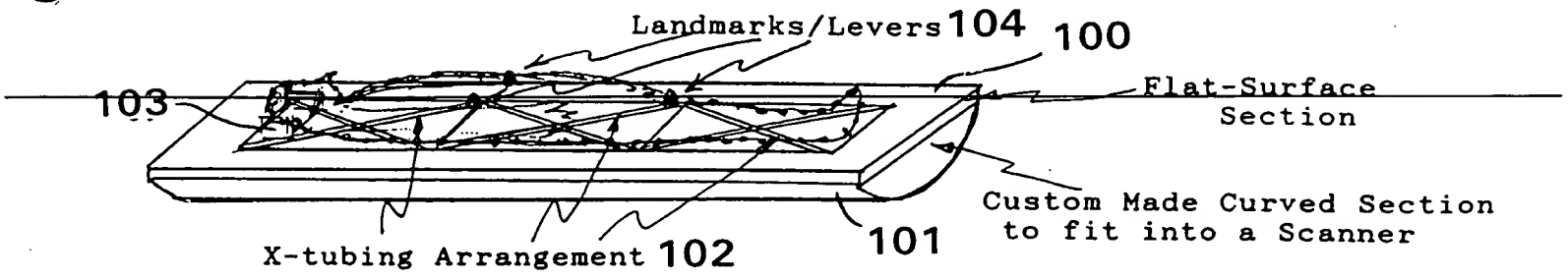
Landmarks/Levers 104
100
103
Flat-Surface Section
Custom Made Curved Section to fit into a Scanner
X-tubing Arrangement 102
101

Fig. 7

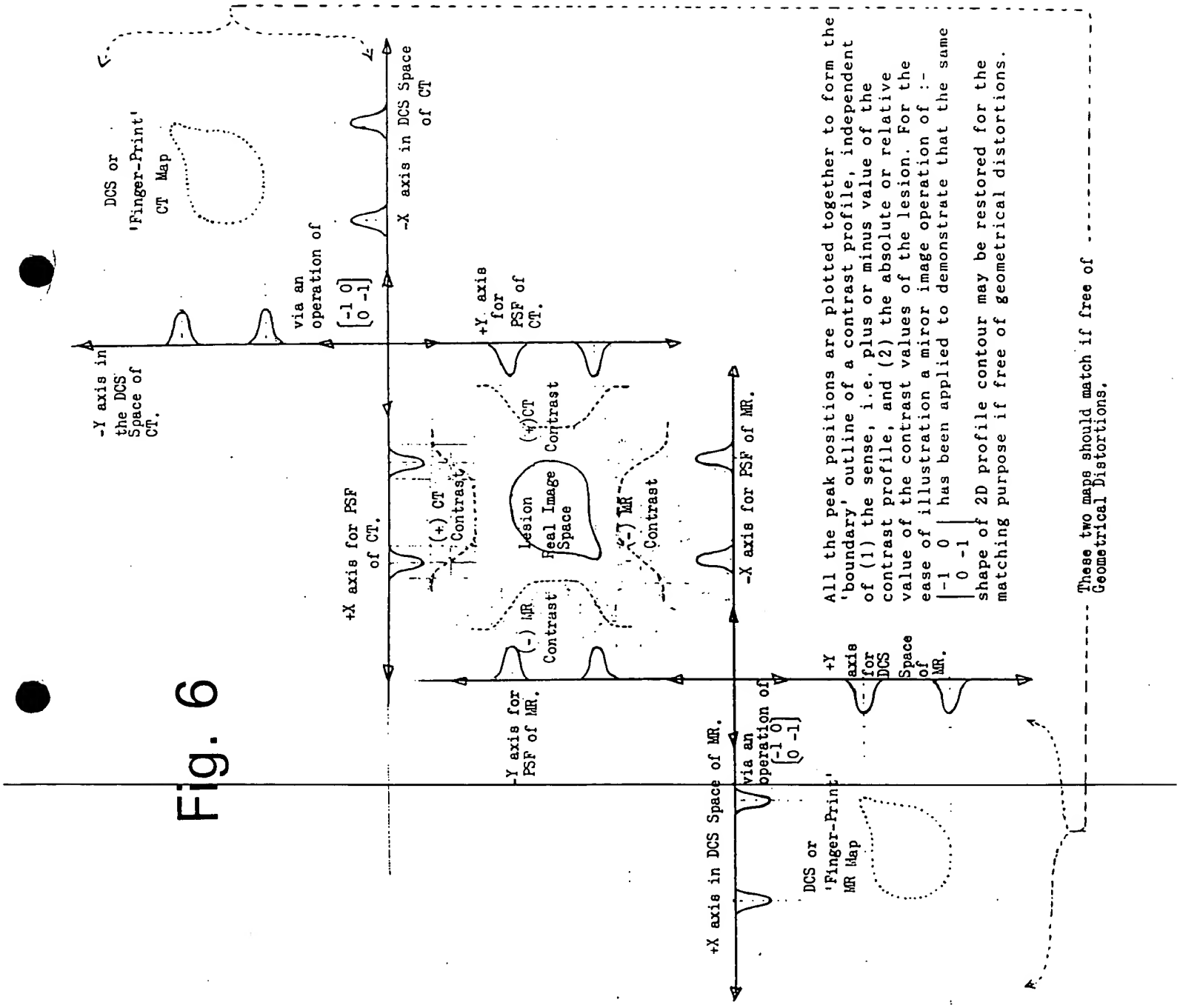
DCS or
'Finger-Print'
CT Map
via an
operation of
[-1 0]
[0 -1]
-X axis in DCS Space
of CT
-Y axis in
the DCS
Space of
CT.
+Y axis
for
PSF of
CT.
+X axis for PSF
of CT.
(+) CT
Contrast
(+)CT
Contrast
Lesion
Real Image
Space
(-) MR
Contrast
(-) MR
Contrast
-X axis for PSF of MR.
-Y axis for
PSF of MR.
+Y
axis
for
DCS
Space
of
MR.
via an
operation of
[-1 0]
[0 -1]
+X axis in DCS Space of MR.
DCS or
'Finger-Print'
MR Map
All the peak positions are plotted together to form the
'boundary' outline of a contrast profile, independent
of (1) the sense, i.e. plus or minus value of the
contrast profile, and (2) the absolute or relative
value of the contrast values of the lesion. For the
ease of illustration a miror image operation of :-
|-1 0 |
| 0 -1 |
has been applied to demonstrate that the same
shape of 2D profile contour may be restored for the
matching purpose if free of geometrical distortions.
These two maps should match if free of
Geometrical Distortions.

Fig. 6

Fig. 8

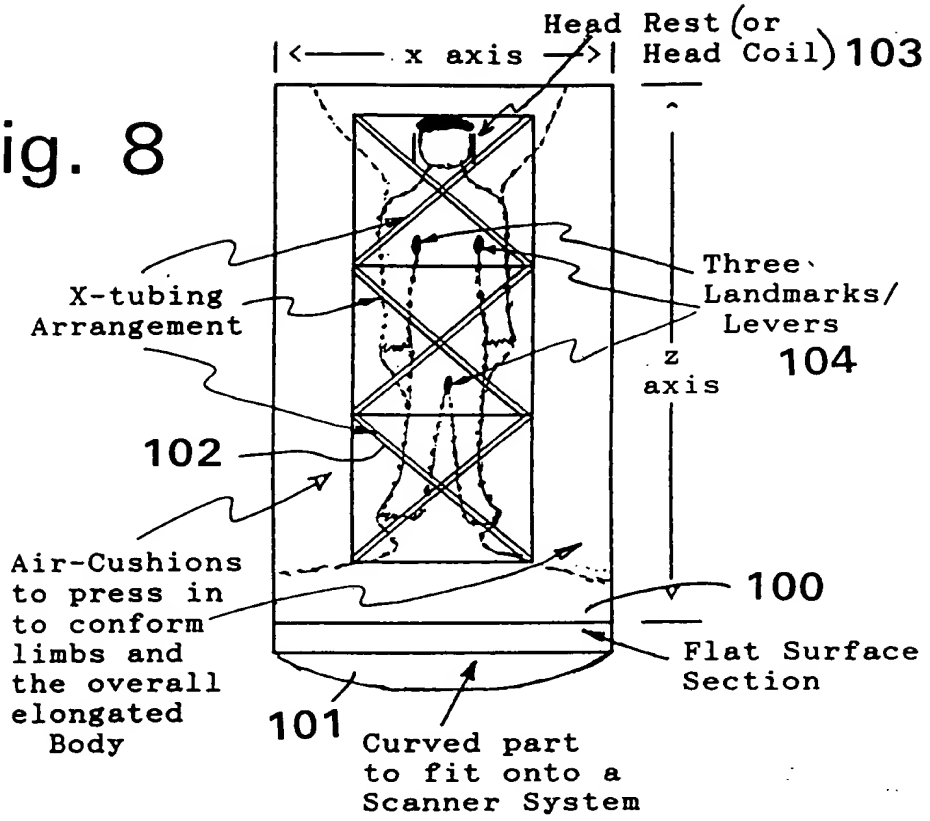
Head Rest (or Head Coil) 103
x axis
X-tubing Arrangement
Three Landmarks/ Levers
104
z axis
102
Air-Cushions to press in to conform limbs and the overall elongated Body
100
Flat Surface Section
101
Curved part to fit onto a Scanner System

Fig. 9

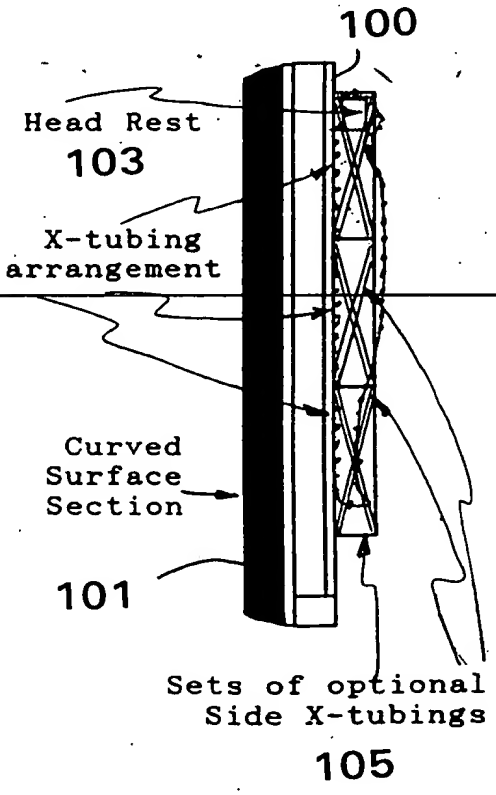
100
Head Rest
103
X-tubing arrangement
Curved Surface Section
101
Sets of optional Side X-tubings
105

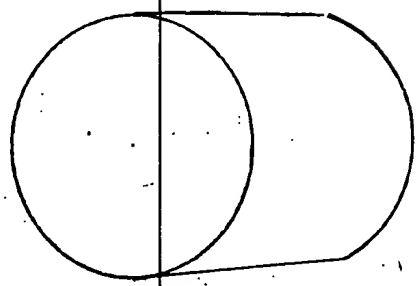

Fig. 10

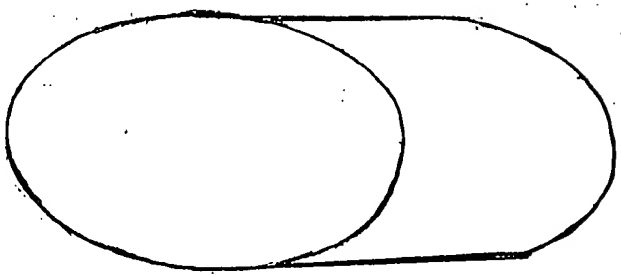

Fig. 12

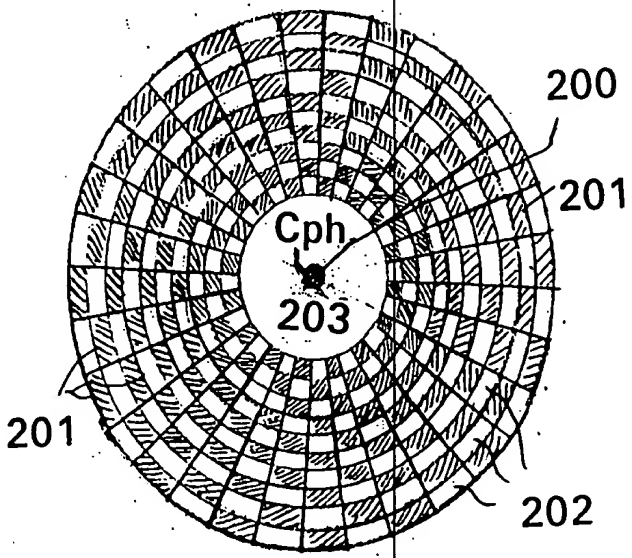

Fig. 11

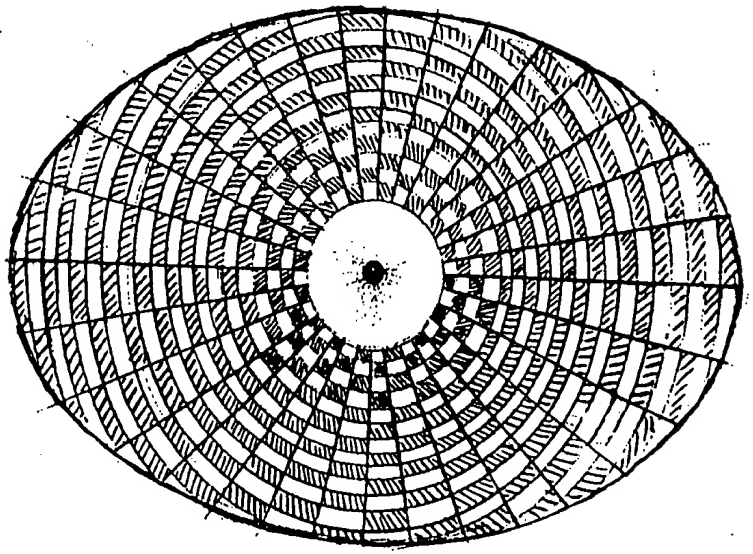

Fig. 13

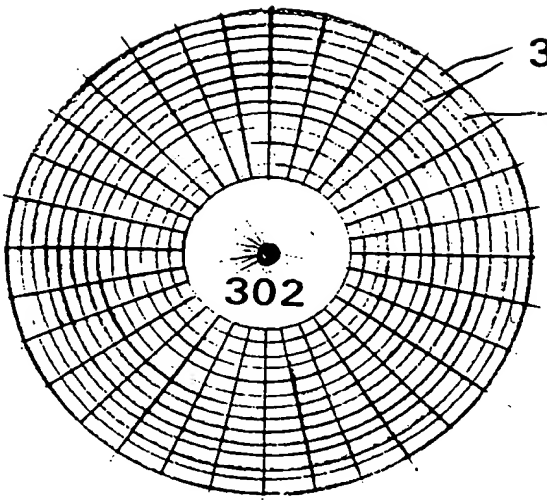

Fig. 14

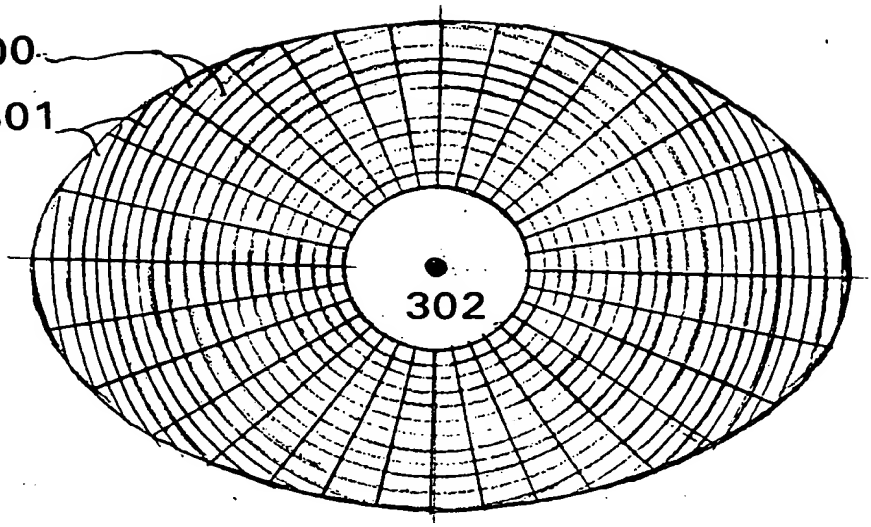

Fig. 15

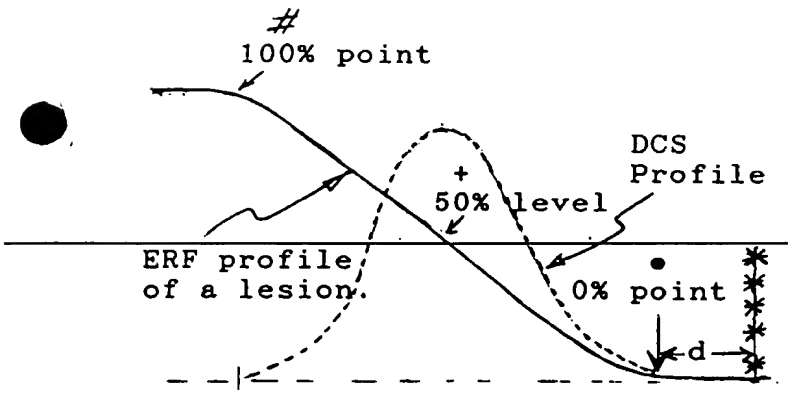

Fig. 16

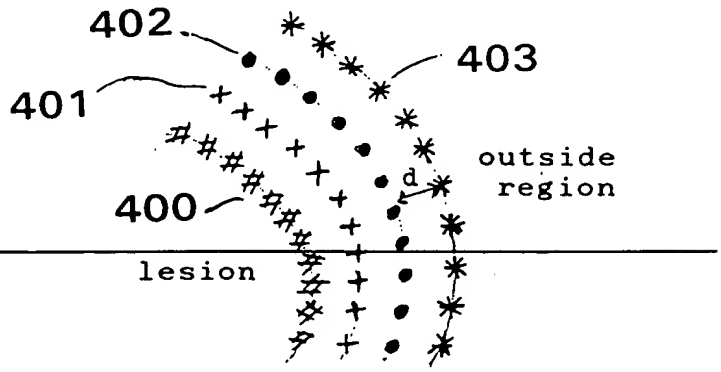

Fig. 17

PCT/GB99/03417

8.11.99

Graham Coles & Co

SANDRINE